and Cellular Biosciences, University of Tokyo, 1-1-1 Yayoi, Bunkyo-ku, Tokyo 113-0032, Japan. e-mail: miyajima@iam.u-tokyo.ac.jp; fax: (81) 3-5841-8475.

Acknowledgments

The authors thank Dr R. Nishinakamura and Dr S. Kawamata for providing us with $WT1^{+/-}$ mice and anti-ALCAM antibody, respectively, and Drs J. James, T. Itoh, N. Tanimizu, and H. Nonaka for valuable discussions and critical reading of the manuscript.

Transcript profiling (expression microarray): National Center for Biotechnology Information Gene Expression Omnibus accession no. GSE 18937. (http://www.ncbi.nlm.nih.gov/geo/query/acc.cgi?acc=GSE18937).

Conflicts of interest

The authors disclose no conflicts.

Funding

Supported in part by a research grant from the Ministry of Health, Labor and Welfare and Grant-in-Aid for Scientific Research and Global COE Project of the Ministry of Education, Culture, Sports, Science and Technology of Japan.

Supplementary Materials and Methods

Antibodies

Goat anti-mouse PCLP1 polyclonal Ab and rabbit anti-mouse Ki67 polyclonal Ab used for IHC were purchased from R&D Systems, Inc. Phycoerythrin-conjugated or biotinylated anti-mouse PCLP1 monoclonal Ab (clone 10B9) used for flow cytometry was supplied from Medical & Biological Laboratories, Co, Ltd (Nagoya, Japan). Biotinylated anti-mouse Msln monoclonal Ab (clone B35) for both IHC and flow cytometry was prepared as described previously.[1] Anti-mouse delta-like 1 homologue (Dlk1) monoclonal Ab[2] was biotinylated by ECL Protein Biotinylation Module (GE Healthcare, Tokyo, Japan) according to the manufacturer's protocol. Other fluorescently labeled Abs and anti-FcγR Ab used for flow cytometry were purchased from Pharmingen (San Diego, CA). To detect signals of biotinylated Abs in flow cytometry, allophycocyamin-conjugated streptavidin (BioLegend, San Diego, CA) was used.

IHC

Whole embryos or livers dissected from animals were frozen and cryosectioned into 6-μm slices. Sections were fixed with 4% paraformaldehyde in phosphate-buffered saline for 10 minutes at room temperature, followed by incubation with each primary Ab. Sections were incubated with fluorescently labeled secondary antibodies to detect signals by fluorescence microscopy. Ki67 immunocytochemistry was performed using PCLP1^{high} MCs sorted from E13.5 livers by a cell sorter. Cytospin samples were fixed and immunostained using Ki67 Ab as described previously.

Quantitative RT-PCR Analysis

Total RNA was extracted from cells by using TRIzol reagent (Invitrogen, Carlsbad, CA). First-strand complementary DNA was synthesized using a High Capacity cDNA Reverse Transcription Kit (Applied Biosystems, Foster City, CA) and was used as a template for PCR amplification. The primer sequences used are as follows: *GAPDH*, 5′-TGAACGGGAAGCTCACTGG-3′ and 5′-TCCACCACCCTGTTGCTGTA-3′; *Msln*, 5′-CTATCCTGAGTCCCTGATCCA-3′ and 5′-TCGCCTGAGCATTCATCTTT-3′; *HGF*, 5′-CCCGAGAACTTCAAATGCAA-3′ and 5′-TATGACGGTGTAAATCCTCCA-3′; *Ptn*, 5′-GGAAGAAGCAGTTTGGAGCTG-3′ and 5′-GGCGGTATTGAGGTCACATTC-3′; *Mdk*, 5′-TGATGGGAGCACTGGCAC-3′ and 5′-CATTGTACCGCGCCTTCTT-3′; *PCLP1*, 5′-GCAAGAGCGGTGACAGTTTTA-3′ and 5′-AGTTGTCAGTGCTGGGCGT-3′; *Msln*, 5′-CTATCCTGAGTCCCTGATCCA-3′ and 5′-TCGCCTGAGCATTCATCTTT-3′; *WT1*, 5′-CAGATGAACCTAGGAGCTACCTTAAA-3′ and 5′-CGTGGTTGCTCTGCCCTTCT-3′; *Raldh2*, 5′-CATGGTATCCTCCGCAATG-3′ and 5′-GCGCATTTAAGGCATTGTAAC-3′. The real-time PCR reactions were performed using LightCycler (Roche Diagnostics KK, Toyko, Japan) according to the manufacturer's protocol.

In Vitro Colony Formation Assay

MCs were prepared by sorting of Flk1^{-}PCLP1^{high} cells using EPICS ALTRA from E12.5 livers or by sorting of Msln^{+} cells using autoMACS or EPICS ALTRA from E18.5, PD7, or adult livers. MCs (1×10^3 cells) were then inoculated into each well of a type IV collagen–coated 6-well plate (AGC Techno Glass, Chiba, Japan) and cultured in α–minimum essential medium (Invitrogen) containing 10% fetal bovine serum (JRH Biosciences, Tokyo, Japan) and 50 nmol/L mercaptoethanol (Invitrogen). After 6 days of culture, the plates were stained with Giemsa solution (Merck, Damstadt, Germany) to visualize the cells and colonies were counted under the microscope. Averages of 3 wells from each sample were used to evaluate cell proliferation.

References

1. Rump A, Morikawa Y, Tanaka M, et al. Binding of ovarian cancer antigen CA125/MUC16 to mesothelin mediates cell adhesion. J Biol Chem 2004;279:9190–9198.
2. Tanaka M, Okabe M, Suzuki K, et al. Mouse hepatoblasts at distinct developmental stages are characterized by expression of EpCAM and DLK1: drastic change of EpCAM expression during liver development. Mech Dev 2009;126:665–676.

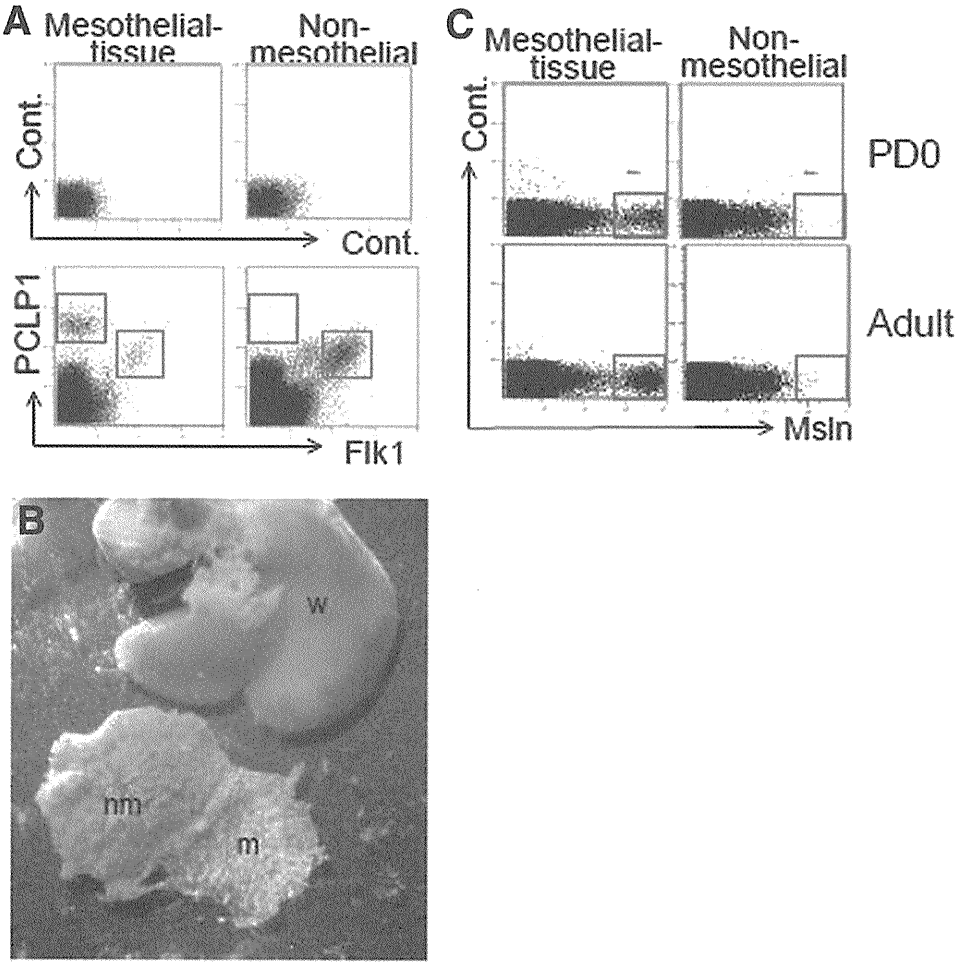

Supplementary Figure 1. (*A*) FCM of E16.5 liver cells with anti-PCLP1 and anti-Flk1 Abs. *Red* and *green lines* in *lower panels* indicate PCLP1^{high} and PCLP1^{med} cell populations, respectively. Note that Flk1^{-}PCLP1^{high} cells were present exclusively in the mesothelial tissue, while Flk1^{+}PCLP1^{med} cells were detected mainly in the non-mesothelial tissue. (*B*) Appearance of surgically separated adult liver mesothelial tissue (m) and non-mesothelial tissue (nm). w, non-separated whole liver. (*C*) FCM with anti-Msln Ab using neonatal (PD0) or adult liver cells. *Red lines* in each *panel* indicate Msln^{+} cell population. Note that the cells highly expressing Msln are exclusively detected in the surgically separated mesothelial tissue in PD0 and adult livers.

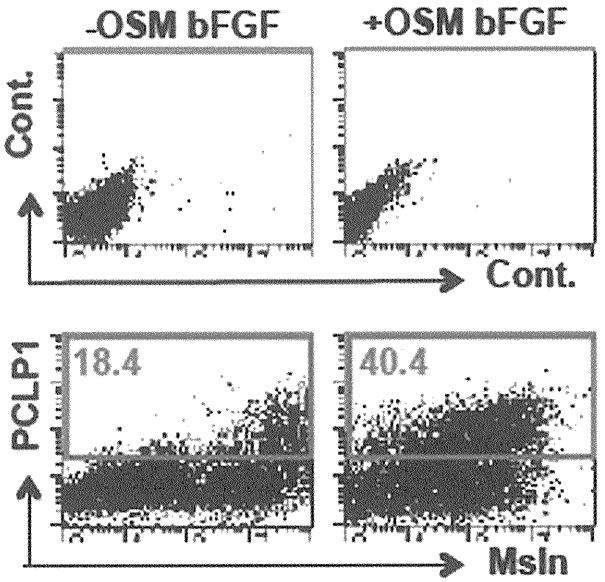

Supplementary Figure 2. FCM of cultured MCs with anti-PCLP1 and anti-Msln Abs. After first passage of cultured E12.5 Flk1^{-}PCLP1^{high} cells in the presence of OSM and bFGF, the cells were incubated for additional 6 days in the presence or absence of the cytokines, followed by FCM. *Red lines* and numbers in *lower panels* indicate PCLP1^{+} cell populations and their percentages, respectively.

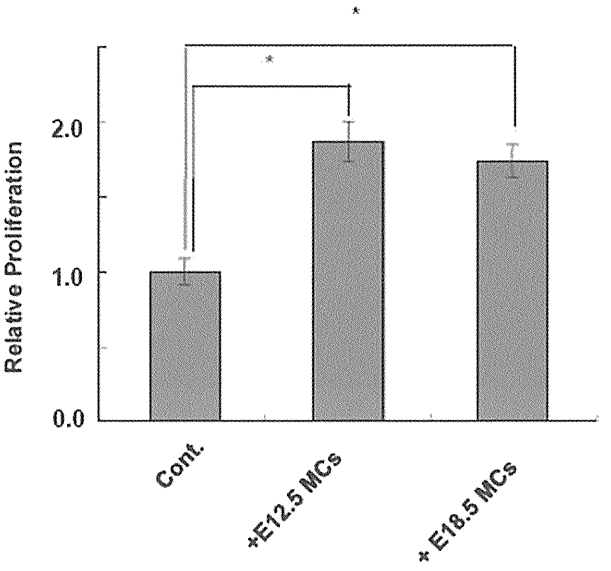

Supplementary Figure 3. Proliferation of E14.5 Dlk1^{+} cells cultured with in vitro expanded MCs from E12.5 or E18.5 livers. Growth of hepatocytes was measured by WST-1 assay after 3 days of coculture. Averages of 3 wells for each sample are shown. *$P < .005$; Student *t* test.

Supplementary Table 1. Growth Factors Preferentially Expressed in Immature MCs

Genbank	Gene symbol	Description	E12.5 PCLP1highMsln^{-}	Adult Msln^{+}	E12.5/Adult Ratio
AV240088	Fgf5	Fibroblast growth factor 5	413.0	1.0	>100.0
NM_010514	Igf2	Insulin-like growth factor 2	226.3	1.4	>100.0
BC002064	Ptn	Pleiotrophin	2129.3	18.1	80.0
U50279	Vegfa	Vascular endothelial growth factor A	79.7	0.8	68.3
AV269710	Angpt4	Angiopoietin 4	124.7	2.0	42.6
M34328	Mdk	Midkine	9680.6	158.6	41.5
AF020737	Fgf13	Fibroblast growth factor 13	198.8	4.1	32.9
NM_019971	Pdgfc	Platelet-derived growth factor, C polypeptide	2805.1	58.1	32.8
NM_008243	Mst1	Macrophage stimulating 1 (hepatocyte growth factor-like)	75.0	1.6	31.5
NM_010514	Igf2	Insulin-like growth factor 2	12,753.5	285.0	30.4
NM_019971	Pdgfc	Platelet-derived growth factor, C polypeptide	3830.3	109.1	23.9
BC002064	Ptn	Pleiotrophin	878.0	26.0	22.9
NM_009704	Areg	Amphiregulin	20.2	0.7	19.7
NM_009521	Wnt3	Wingless-related MMTV integration site 3	5.5	0.2	16.0
AU015375	Bmp15	Bone morphogenetic protein 15	12.7	0.6	15.5
NM_010201	Fgf14	Fibroblast growth factor 14	14.9	1.0	10.1
AV032115	Bmp5	Bone morphogenetic protein 5	133.8	9.6	9.4
AB073819	Wnt9b	Wingless-type MMTV integration site 9B	14.8	1.2	8.6
BB476818	Hgf	Hepatocyte growth factor	143.2	12.9	7.5
AB016516	Fgf5	Fibroblast growth factor 5	26.6	2.5	7.3
AK003506	Il17b	Interleukin 17B	35.1	3.6	6.6
NM_009505	Vegfa	Vascular endothelial growth factor A	660.0	75.6	5.9
NM_021782	Il21	Interleukin 21	15.7	1.9	5.6
NM_021380	Il20	Interleukin 20	67.4	8.8	5.2
BM210179	Bmp8b	Bone morphogenetic protein 8b	22.9	3.0	5.2

NOTE. Microarray analysis was performed using E12.5 PCLP1^{high}Msln^{-} immature MCs and adult mature Msln^{+} MCs. The list shows growth factors whose expression in E12.5 MCs is more than 5 times higher than adult MCs.

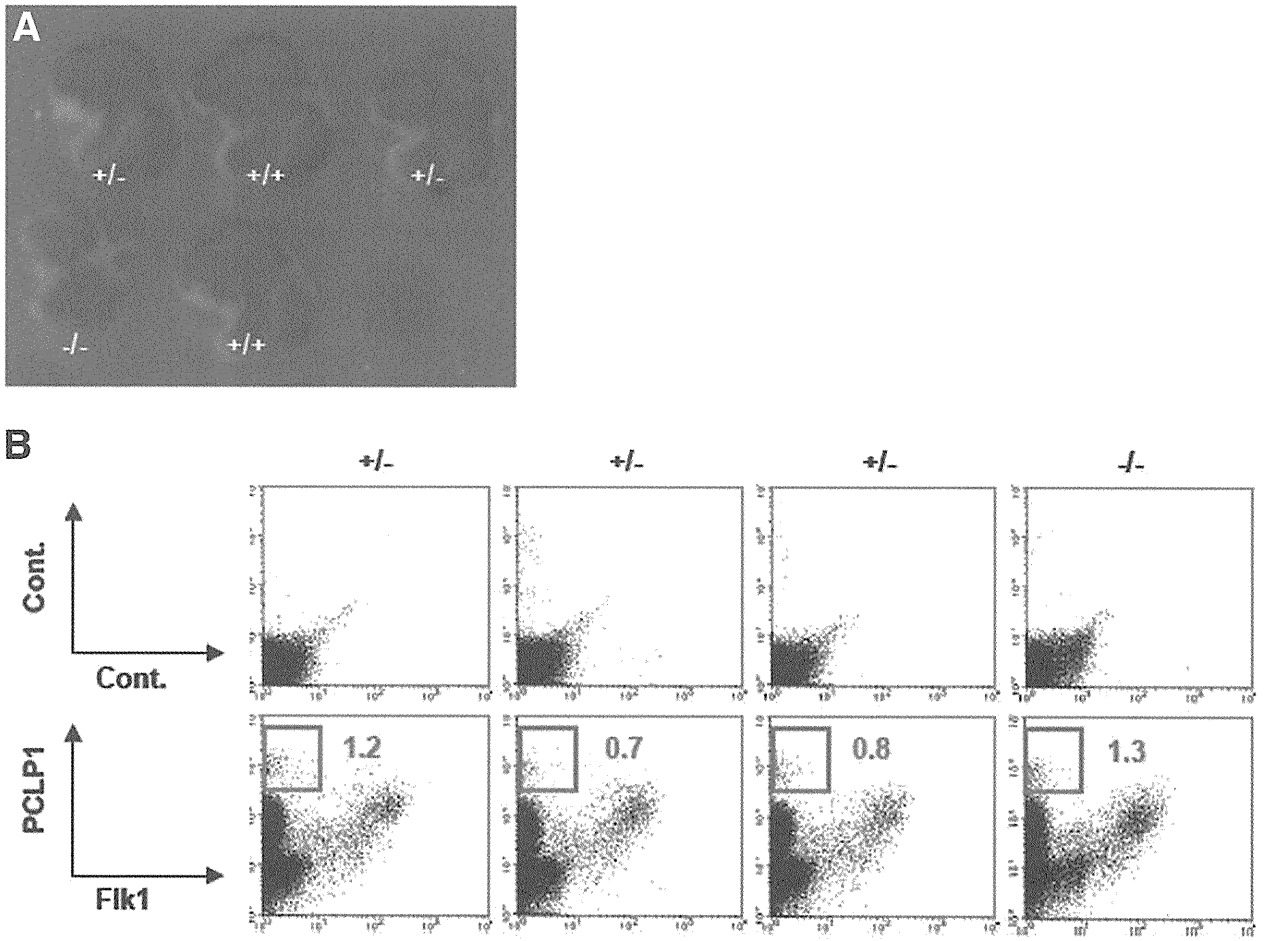

Supplementary Figure 4. (*A*) The morphology of E13.5 livers from littermates with each genotype. Note that the liver of $WT1^{-/-}$ embryo is smaller than those of the other littermates. (*B*) FCM of E13.5 liver cells from each littermate with anti-Flk1 and anti-PCLP1 Abs. The genotypes are indicated above each *panel*. *Red lines* and numbers in the *lower panels* indicate $Flk\text{-}1^{-}PCLP1^{high}$ cells and its percentages, respectively. Note that $Flk1^{-}PCLP1^{high}$ cells are detected in $WT1^{-/-}$ FLs as well as $WT1^{+/-}$ littermates.

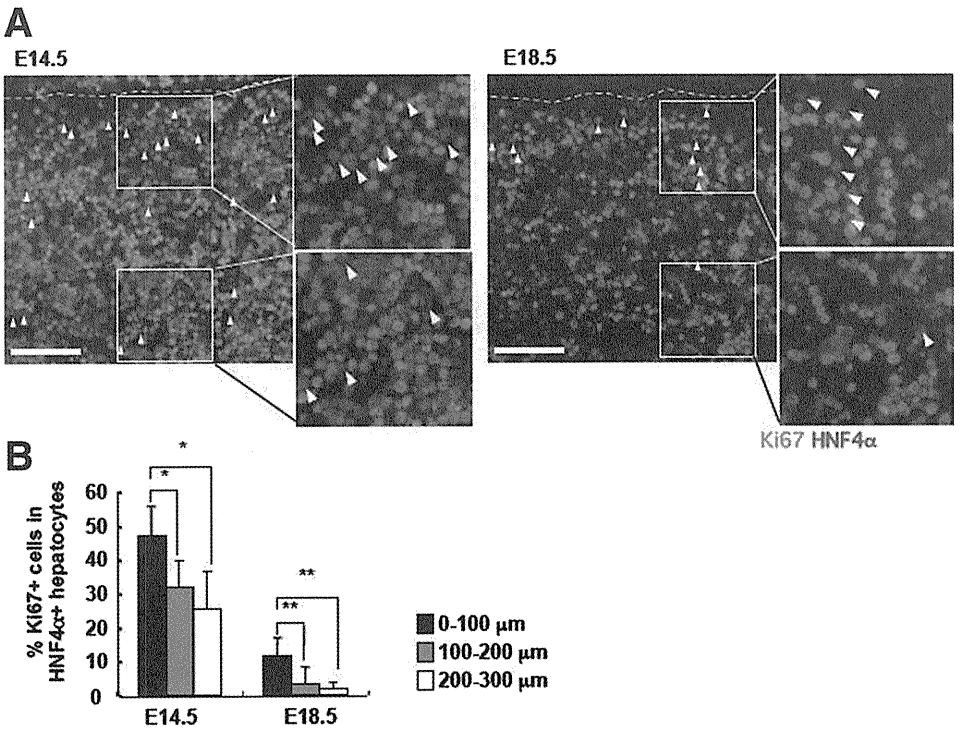

Supplementary Figure 5. Distribution of proliferating hepatocytes in the developing liver (*A*) immunostaining of E12.5 and E18.5 FL sections with anti-Ki67 (*green*) and anti-HNF4α (*red*) Abs. The *dotted lines* in the *left panels* indicate MC layer. Higher magnified images of *boxed areas* are shown in the *right*. The *arrowheads* indicate Ki67+HNF4α+ cells. Note that Ki67$^+$HNF4α$^+$ cells are observed more abundantly in the peripheral regions than in the central regions of hepatic lobes. *Scale bars*, 80 μm. (*B*) The percentages of Ki67$^+$ cells in HNF4α$^+$ cells in each 100 × 300 μm^2 area at 0–100, 100–200, and 200–300 μm distance from the MC layer. Microscopic views of 300 μm × 300 μm were used for analyses (E14.5, n = 5; E18.5, n = 12). *$P < .05$; **$P < .005$; Student *t* test.

Supplementary Table 2. The Number of HNF4α$^+$ cells Used for Analysis

	Number of HNF4α$^+$ cell in each 100 × 300 μm^2 area		
	0–100 μm	100–200 μm	200–300 μm
E14.5 (n* = 5)	38.4 ± 8.3 (47.2 ± 8.7)	38.8 ± 9.5 (32.1 ± 8.0)	35.2 ± 5.0 (25.4 ± 11.3)
E18.5 (n* = 12)	56.9 ± 10.9 (11.5 ± 5.4)	58.4 ± 7.0 (3.2 ± 5.0)	52.9 ± 8.0 (1.7 ± 2.0)

NOTE. The number of HNF4α$^+$ cells in each 100 × 300 μm^2 area at 0–100, 100–200, and 200–300 μm distance from the MC layer was counted for Supplementary Figure 4*B*. The percentages of Ki67$^+$ cells in HNF4α$^+$ cells are shown in parentheses. n*, number of 300 μm × 300 μm views.

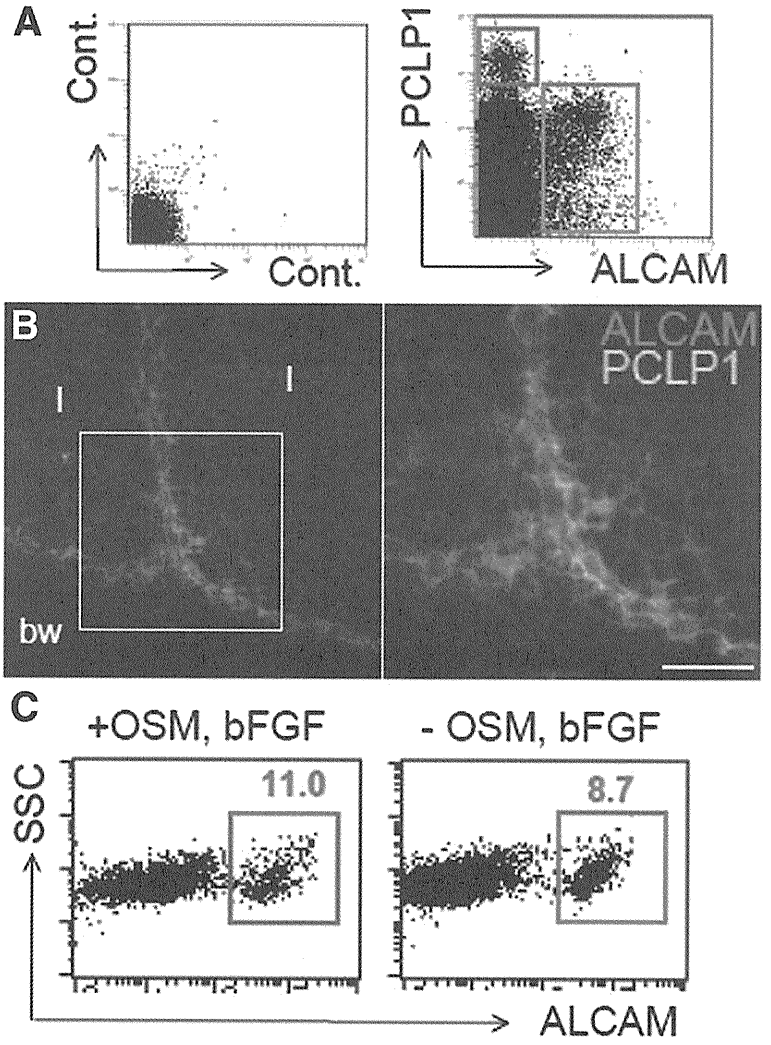

Supplementary Figure 6. (*A*) FCM of E12.5 liver cells using fluorescently labeled Abs against ALCAM and PCLP1. *Red* and *green lines* in the *right panel* indicate PCLP1^{high} cells and ALCAM^{+} cells, respectively. Note that PCLP1^{high} cells are negative for ALCAM. (*B*) IHC on E13.5 liver sections with anti-ALCAM (*red*) and anti-PCLP1 (*green*) Abs. Higher magnification image of the *boxed region* in the *left panel* is shown in the *right panel*. Note that PCLP1^{+} MC layers and ALCAM^{+} submesothelial layers are clearly distinguishable. l, lobe; bw, body wall. *Scale bar*, 40 μm. (*C*) FCM of cultured MCs using fluorescently labeled Abs against ALCAM. PCLP1^{high} cells sorted from E12.5 FL were cultured in the presence of OSM and bFGF, and further cultured for 3 days in the presence or absence of OSM and bFGF. Note that ALCAM^{-}PCLP1^{high} immature MCs give rise to ALCAM^{+} cells in vitro.

Biochemical and Biophysical Research Communications 379 (2009) 817–823

Contents lists available at ScienceDirect

Biochemical and Biophysical Research Communications

journal homepage: www.elsevier.com/locate/ybbrc

Hematopoiesis-dependent expression of CD44 in murine hepatic progenitor cells

Shinya Ohata [a,b,c], Makiko Nawa [d], Takeshi Kasama [d], Tokiwa Yamasaki [a,b], Kenji Sawanobori [a,b], Shoji Hata [a], Takashi Nakamura [a], Yoichi Asaoka [a], Toshio Watanabe [e], Hitoshi Okamoto [c], Takahiko Hara [f], Shuji Terai [g], Isao Sakaida [g], Toshiaki Katada [b], Hiroshi Nishina [a,*]

[a] Department of Developmental and Regenerative Biology, Medical Research Institute, Tokyo Medical and Dental University, Tokyo, 1-5-45 Yushima, Bunkyo-ku, Tokyo 113-8510, Japan
[b] Department of Physiological Chemistry, Graduate School of Pharmaceutical Sciences, University of Tokyo, Tokyo, Japan
[c] Laboratory for Developmental Gene Regulation, RIKEN Brain Science Institute, Saitama, Japan
[d] Laboratory of Cytometry and Proteome Research, Tokyo Medical and Dental University, Tokyo, Japan
[e] Graduate School of Humanities and Sciences School of Natural Science and Ecological Awareness, Nara Women's University, Kitauoyahigashi-machi, Nara, Japan
[f] Department of Tumor Biochemistry, The Tokyo Metropolitan Institute of Medical Science, Tokyo, Japan
[g] Department of Gastroenterology and Hepatology, School of Medicine, Yamaguchi University, Yamaguchi, Japan

ARTICLE INFO

Article history:
Received 25 November 2008
Available online 3 January 2009

Keywords:
Liver
Hepatogenesis
Hepatoblast
Hematopoiesis
Monoclonal antibody
Liv8
CD44
AML1
AGM
Erythrocyte
Liver development

ABSTRACT

The fetal liver serves as the predominant hematopoietic organ until birth. However, the mechanisms underlying this link between hematopoiesis and hepatogenesis are unclear. Previously, we reported the isolation of a monoclonal antibody (anti-Liv8) that specifically recognizes an antigen (Liv8) present in murine fetal livers at embryonic day 11.5 (E11.5). Liv8 is a cell surface molecule expressed by hematopoietic cells in both fetal liver and adult mouse bone marrow. Here, we report that Liv8 is also transiently expressed by hepatoblasts at E11.5. Using protein purification and mass spectrometry, we have identified Liv8 as the CD44 protein. Interestingly, the expression of Liv8/CD44 in fetal liver was completely lost in *AML1*$^{-/-}$ murine embryos, which lack definitive hematopoiesis. These results show that hepatoblasts change from Liv8/CD44-negative to Liv8/CD44-positive status in a hematopoiesis-dependent manner by E11.5, and indicate that Liv8/CD44 expression is an important link between hematopoiesis and hepatogenesis during fetal liver development.

Fetal liver is known to serve as the predominant hematopoietic organ during its own proliferation and differentiation until birth [1]. Hepatogenesis and hematopoiesis have close interactions as follow. Hepatoblasts, which are hepatic progenitor cells, are thought to support hematopoiesis because hepatocyte-like cell lines were reported to be able to support hematopoiesis [2,3]. On the other hand CD45-positive (CD45^{+}) hematopoietic cells in the fetal liver produce an Interleukin-6 (IL-6) family cytokine, Oncostatin M (OSM), to promote the development of hepatocytes in the middle to late liver development [4,5]. However, the molecules linking hepatogenesis and hematopoiesis during early fetal liver development remains unknown.

The process of embryonic liver development can be divided into several distinct stages [6]. The liver primordium proliferates and invades the septum transversum mesenchyme to give rise to the hepatic codes and buds at E9.5. Hepatic cells at this stage, called hepatoblasts, possess the potential to differentiate into both parenchymal hepatocytes and bile duct epithelial cells. At around E10.5, hematopoietic stem cells originating from aorta–gonad–mesonephros (AGM) region colonize the fetal liver and expand their mass and lineage diversity, such as erythrocytes [1,7]. Hepatoblasts participate in creating the hematopoietic microenvironment in concert with other stromal cells to promote embryonic hematopoiesis [2,3].

We have prepared several monoclonal antibodies specifically recognizing murine fetal livers because molecular markers and tools were needed to understand the mechanisms of early liver development [8,9]. One of the antibodies, called anti-Liv2,

* Corresponding author. Fax: +81 3 5803 5829.
E-mail address: nishina.dbio@mri.tmd.ac.jp (H. Nishina).

0006-291X/$ - see front matter © 2008 Elsevier Inc. All rights reserved.
doi:10.1016/j.bbrc.2008.12.149

recognized hepatoblasts specifically at E9.5–E12.5. We could analyzed hepatoblast proliferation in knockout mice using anti-Liv2 [9,10]. Furthermore, we have reported another antibody, anti-Liv8, that recognize both hematopoietic progenitor cells in fetal liver at E11.5 and CD45$^+$ hematopoietic cells in adult bone marrow [11,12]. However, its molecular identification of the Liv8-antigen (Liv8) and its expression in embryonic development were remained unknown.

In this report, we show a molecular identification of Liv8 as CD44. Our finding suggest that Liv8/CD44 links hematopoiesis and hepatogenesis by its the adhesive activity and signaling role during fetal liver development.

Materials and methods

Mice. C57BL/6J mice were purchased from CLEA Japan. *AML1* mutant mice were generated as described previously [13].

Antibodies. Anti-Liv2 and anti-Liv8 antibodies were prepared and purified as described [9]. Anti-Liv8 antibody was biotinylated by using EZ link Sulfo-NHS-Biotin (Pierce) and anti-Liv2 antibody was labeled with Alexa Fluor 488 by using Zenon labeling kit (Invitrogen). Fluorescein isothiocyanate (FITC)-conjugated and unconjugated anti-CD44 (IM7 and KM114), FITC-conjugated anti-CD71 (C2) and phycoerythrin (PE)-conjugated anti-TER-119 antibodies were purchased from Becton Dickinson Biosciences, anti-Myc (9E10) and anti-FLAG (M2) antibodies were from Sigma, anti-Glyceraldehyde-3-phosphate dehydrogenase (GAPDH, 6C5) antibody was from CHEMICON.

Immunohistochemistry. Paraffin-embedded and frozen sections were immunostained according to previously described protocols [9].

Cell culture and transfection. LO cells were established as described previously [14], and maintained in Dulbecco's modified Eagle medium (DMEM, Invitrogen) supplemented with 15% fetal calf serum (FCS), 10 ng/mL mouse OSM (Sigma) and antibiotics. cDNA encoding CD44 tagged with FLAG at C-terminal (FLAG-CD44) were cloned into mammalian expression vector pCMV5. For gene expression analysis, 293T cells were plated and transfected 1 day later with 5 μg of plasmid DNA using LipofectAMINE 2000 (Invitrogen).

Immunoblotting. Fetal liver (E11.5), LO and COS-7 cells were washed and homogenized in phosphate-buffered saline (PBS). The homogenates were centrifuged at 900*g* for 10 min at 4 °C, and the supernatants were centrifuged at 100,000*g* for 30 min at 4 °C. The resulting membrane pellets were used as membrane fractions. For the deglycosylation of membrane fraction, samples were incubated with PNGase F (PROzyme) or neuraminidase (nacalai tesque) according to the manufacturer's instructions. Immunoprecipitation and immunoblotting were performed as described [15].

Purification of Liv8-antigen and mass spectrometry. LO membrane fraction was lysed in 50 mM Tris–HCl (pH 7.5), 1% Lubrol PX (lysis buffer), and centrifuged at 100,000*g* at 4 °C for 1 h. The supernatant was applied on WGA agarose column (Seikagaku Corporation) equilibrated with lysis buffer. The column was washed with 1 mM phosphate buffer (pH 7.4), 1 M NaCl, 0.1% sodium-cholate (wash buffer), and the protein was eluted with wash buffer containing 250 mM N-acetyl-D-glucosamine (GlcNAc). The GlcNAc eluant was then applied on Phenyl-Sepharose column (GE healthcare) equilibrated with wash buffer, and the protein was eluted with a liner gradient of 1000–0 mM NaCl and 0.1–2% of sodium-cholate. The Liv8-positive fractions were adjusted to 1 mM $CaCl_2$, then applied on the hydroxyapatite Bio-Gel HTP Gel column (Bio-Rad) equilibrated with 1 mM phosphate buffer, 0.3 mM $CaCl_2$, 0.1 % Lubrol PX. The protein was eluted with a liner gradient of 1–400 mM phosphate containing 0.1% Lubrol PX and 0.1 mM EDTA. The Liv8-positive fractions were diluted with 50 mM Tris–HCl (pH 7.5), 0.1% Lubrol PX (dilution buffer) and applied on Mono Q HR5/5 column (GE healthcare) equilibrated with dilution buffer. The protein was eluted with a liner gradient of 0–1 M NaCl in dilution buffer. Purified Liv8-antigen was concentrated with VIVASPIN (VIVASCIENCE) and separated by SDS–PAGE. The proteins were visualized with Silver Stain II Kit Wako or negative gel stain MS kit according the manufacturer's instructions (Wako). The appropriate position was cut out and washed with 5% acetate, 50% methanol, and dehydrated with 66% acetonitrile, 17 mM NH_4HCO_3. The protein was reduced by 10 mM dithiothreitol, alkylated by 55 mM iodoacetamide, and digested by trypsin. The peptide solution was placed on the target tip with α-cyano-4-hydroxy cinnamic acid as the matrix. The spectra of the peptides were obtained using Ultraflex mass spectrometer (BRUCKER) and Voyager DE-STR (Applied Biosystems).

Fluorescence-activated cell sorter (FACS) analysis. Freshly isolated fetal livers were incubated with Liver Perfusion Medium and Liver Digestion Medium (Invitrogen) at 37 °C. The cells were dissociated by pipetting, washed with PBS, and reacted with fluorescein-labeled antibodies according to previously described protocol [11]. The labeled cells were analyzed using FACSCalibur (Becton Dickinson Biosciences).

Results

Expression of Liv8 in murine fetal liver

As almost all cells were Liv8$^+$ in fetal liver at E11.5 (Fig. 1A), we first examined the expression of Liv8 in hepatoblasts, and found that Liv8 is expressed in Liv2$^+$ hepatoblasts in fetal liver at E11.5 (Fig. 1B; arrowheads). Next, we examined the expression of Liv8 in fetal livers during E9.5 to E13.5. Interestingly, Liv8 was not expressed in hepatoblasts at E9.5 (Fig. 1C, dotted line). The ratios of Liv8$^+$ cells in fetal livers transiently increased and reached its maximum at E11.5, and then decreased at E12.5. Thus, hepatoblasts were Liv8$^-$ at E9.5 and became Liv8$^+$ at E11.5.

Previously, we reported that hematopoietic progenitor cells in fetal liver are Liv8$^+$ at E11.5 [11]. So, we next investigated the expression of Liv8 in AGM region, in which adult-type definitive hematopoiesis begins (Supplementary Fig. S1). Endothelial cells in AGM region at E9.5 were Liv8$^+$, and putative hematopoietic cells protruding from dorsal aorta at E11.5 were also Liv8$^+$. These results indicate that hematopoietic progenitor cells are Liv8$^+$ and hepatoblasts change from Liv8$^-$ at E9.5 to Liv8$^+$ at E11.5 in developing fetal livers.

Identification of Liv8 as CD44

To identify Liv8, we screened Liv8$^+$ cell line and found an endothelial-like cell line, LO cell, established from AGM region [14]. A band of molecular weight of 90-kDa recognized by anti-Liv8 antibody was detected in murine fetal liver and LO cells but not COS-7 cells (Fig. 2A). The band was disappeared by incubation with PNGase F that cleaves asparagine-linked oligosaccharides from glycoprotein, and was shifted to low molecular weight side by incubation with sialidase (Supplementary Fig. S2). These results indicate that Liv8-antigen is a 90-kDa glycoprotein, so we screened Liv8-antigen binding lectins and found Liv8-antigen bind to wheat germ agglutinin (WGA), a lectin that binds to hybrid type asparagines-linked oligosaccharides (data not shown). We purified Liv8-antigen from LO cells by various columns including WGA column, using anti-Liv8 blot as an index (see Materials and methods). Purified Liv8 was subjected to mass analysis. The amino acid sequence of

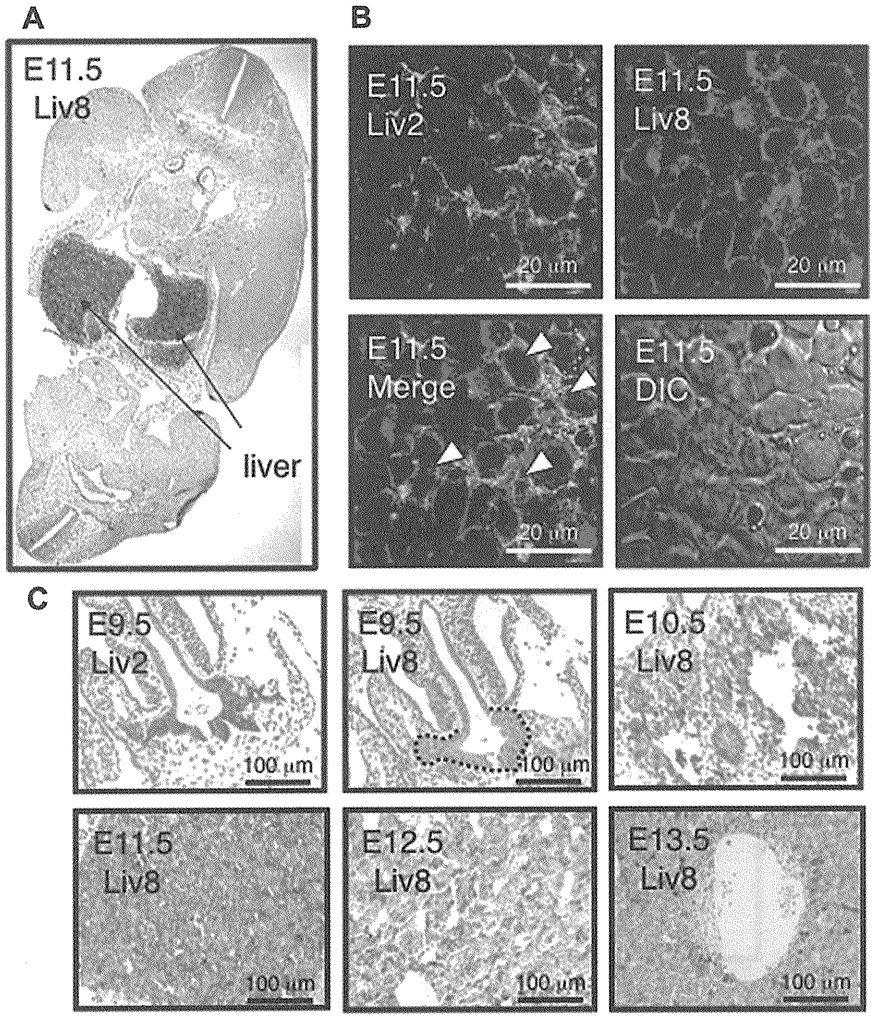

Fig. 1. Expression of Liv8 in murine fetal liver. (A) A transverse paraffin-section of murine embryo at E11.5 was stained with an anti-Liv8 antibody. (B) Transverse frozen section of murine embryonic liver at E11.5 was stained with anti-Liv2 (green) and anti-Liv8 (red) antibodies. Differential interference contrast (DIC) photograph image is also shown. Arrowheads indicate Liv8 expressing hepatoblasts. Scale bars indicate 20 μm. (C) Transverse paraffin-sections of murine embryonic liver at E9.5–13.5 were stained with anti-Liv8 or anti-Liv2 antibodies. Positive cells exhibit a brown precipitate and dotted line indicates hepatic bud at E9.5. Nuclei were counterstained with hematoxylin (purple). Scale bars indicate 100 μm.

spectrum observed at *m/z* 1363.7 from Liv8 was 'YGFIEGNVVIPR' which corresponded to the fragment from CD44.

To examine whether anti-Liv8 antibody recognize CD44, FLAG-CD44 was expressed in 293T cells and analyzed by anti-Liv8 blot (Fig. 2B). Anti-Liv8 and anti-FLAG antibodies recognized FLAG-CD44. Anti-Liv8 antibody also recognized immunoprecipitant of endogenous CD44 from LO cells (Fig. 2C). Finally, E12.5 fetal liver cells were analyzed by FACS using anti-Liv8 and anti-CD44 antibodies, and signals by each antibody were completely coincident (Fig. 2D). These results clearly show that Liv8 is identical to CD44.

Co-localization of Liv8/CD44 and hyaluronic acid in fetal liver but not AGM region at E11.5

CD44 was reported to interact with hyaluronic acid (HA) which is a major component of extra-cellular matrix (ECM) and function in cell adhesion [16]. To examine the interaction between Liv8/CD44 and HA in AGM region and fetal liver, we performed immunohistologic examination of E11.5 embryos using the biotinylated hyaluronic acid binding protein (HABP) and anti-Liv8. Liv8/CD44 and HA did not co-localized in AGM region at E11.5 (Fig. 3A). On the other hand, HA was well co-localized with Liv8/CD44 in fetal liver (Fig. 3B). This result suggests that Liv8/CD44 plays a pivotal role in the adhesion between the hematopoietic cells and hepatoblasts in fetal livers at E11.5.

If Liv8/CD44 functions in hematopoietic cells to adhere with fetal liver, the expression is expected to decrease with their maturation to leave fetal liver. So, we examined changes in Liv8/CD44 expression of hematopoietic cells accompanied with their differentiation to erythroid (Fig. 3C). Erythroid differentiation can be monitored step by step and quantitatively by FACS; this analysis distinguishes CD71 (transferrin receptor) and TER119 (erythroid lineage marker) double-stained erythroblasts into different stages of differentiation [17]. We triple-stained E15.5 fetal liver cells with anti-Liv8, CD71, TER119 antibodies and divided them into five populations by their characteristic staining patterns with anti-CD71 and anti-TER119 antibodies. These cells differentiate from R1 to R5 i.e., $CD71^{high}TER119^{low}$, $CD71^{high}TER119^{meddle}$, $CD71^{high}TER119^{high}$, $CD71^{meddle}TER119^{high}$, and $CD71^{low}TER119^{high}$. Quan-

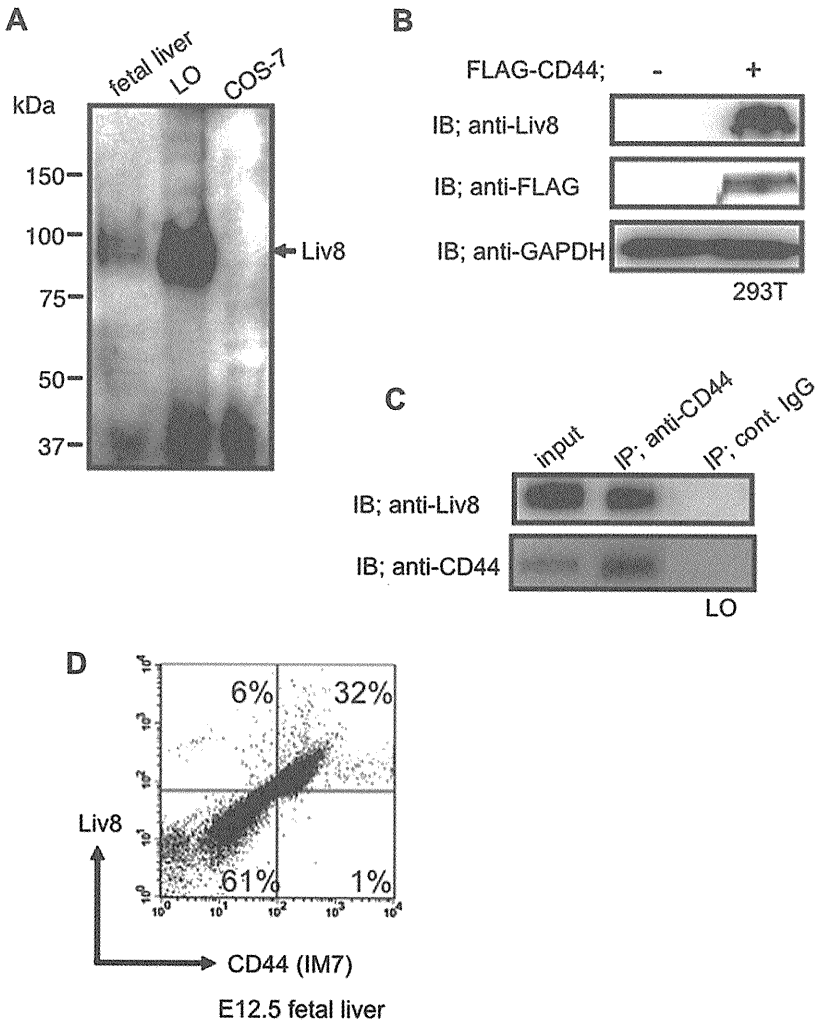

Fig. 2. Identification of Liv8 as CD44. (A) Western blot analysis of Liv8-antigen in fetal liver, LO, and COS-7 cells. (B) FLAG-CD44 or FLAG-peptide alone were expressed in 293T cells. Proteins were separated by SDS–PAGE, and immunoblot was performed with anti-Liv8, anti-CD44 (IM7), and anti-GAPDH antibodies. (C) LO membrane fraction was subjected to immunoprecipitation with anti-CD44 (KM114) antibody or control IgG conjugated resin. Proteins bound to the resin were separated by SDS–PAGE and immunoblotted with anti-Liv8 and anti-CD44 (IM7) antibodies. (D) E12.5 fetal liver cells were stained with FITC-conjugated anti-CD44 and biotin-conjugated anti-Liv8 antibody. The cells were further incubated with allophycicyanin-conjugated streptavidin, and analyzed by FACS. The panel illustrates a plot of fetal liver cells; axes indicate relative logarithmic fluorescence units for FITC (*x*-axis) and allophycicyanin (*y*-axis).

tification of Liv8$^+$ cells of each regions revealed that cells in R1 expressed Liv8/CD44 at high rate, and the rate was decreased gradually from R1 to R5. These results indicate that Liv8/CD44 antigen expression declines gradually during erythropoiesis.

Hematopoiesis-dependent expression of Liv8/CD44 in murine hepatoblasts

To examine the relationship between hematopoiesis and the expression of Liv8/CD44 in hepatoblasts, we utilized *AML1*$^{-/-}$ mice at E11.5, which lack definitive hematopoiesis [13,18]. Interestingly, Liv8/CD44 was expressed in wild-type fetal liver, however, it was completely lost in *AML1*$^{-/-}$ fetal liver (Fig. 4A). On the other hand, Liv8/CD44 was expressed in both wild-type and *AML1*$^{-/-}$ AGM regions (Fig. 4B). These results indicate that an inflow of Liv8/CD44-positive hematopoietic precursor cells into fetal liver is required for the induction of Liv8/CD44 expression in hepatoblasts at E11.5.

Discussion

In the present work, we identified Liv8 as an adhesion molecule CD44 (Fig. 2). We showed that Liv8/CD44 is expressed in hepatoblasts besides hematopoietic progenitor cells in fetal liver (Fig. 1), and the expression of Liv8/CD44 is co-localized with HA in fetal liver at E11.5 (Fig. 3). Furthermore, Liv8/CD44 expression in hepatoblasts is induced in a hematopoiesis-dependent manner (Fig. 4). Our results suggest that Liv8/CD44-positive hematopoietic cells from AGM region to fetal liver induce Liv8/CD44 expression in hepatoblasts at E11.5, and Liv8/CD44 link between hematopoietic cells and hepatoblasts through HA.

CD44 was identified as the major receptor for HA, a component of ECM [16]. It was reported that CD44 expressed by human CD34$^+$ hematopoietic cells and HA expressed in bone marrow sinusoid endothelium and the endosteum region, are essential for homing and repopulation [19]. In the previous and present study, we showed hematopoietic progenitor cells in fetal liver expressed

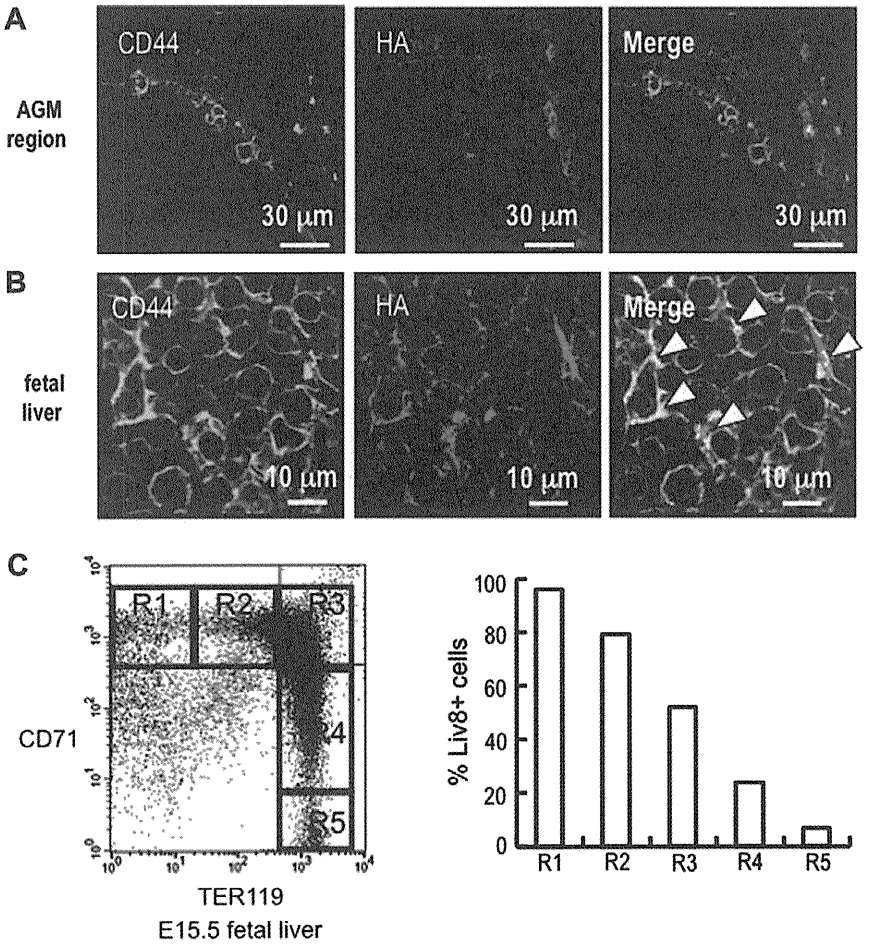

Fig. 3. Expression of Liv8/CD44 and HA in fetal livers. (A,B) Transverse frozen sections of AGM region and fetal liver at E11.5 were stained with anti-Liv8 antibody (green) and HABP (red). Arrowheads indicate co-localization of Liv8-antigen and HA. Scale bars indicate 30 μm (A) and 10 μm (B), respectively. (C) Mouse fetal liver cells were freshly isolated from E15.5 embryos and triple-stained with FITC-conjugated anti-CD71 antibody, PE-conjugated anti-TER119 antibody, and biotin-conjugated anti-Liv8 antibody. Binding of biotin-conjugated anti-Liv8 antibody was detected by using allophycicyanin-conjugated streptavidin. The left panel illustrates a plot of fetal liver cells; axes indicate relative logarithmic fluorescence units for PE (*x*-axis) and FITC (*y*-axis). Regions R1 to R5 are defined by characteristic staining pattern of cells (R1; $CD71^{high}TER119^{low}$, R2; $CD71^{high}TER119^{meddle}$, R3; $CD71^{high}TER119^{high}$, R4; $CD71^{meddle}TER119^{high}$, R5; $CD71^{low}TER119^{high}$). Each region was quantified for expression of Liv8-antigen (right panel).

Liv8/CD44 [11] and HA co-localized with Liv8/CD44 in fetal livers (Fig. 3). Therefore hematopoietic progenitor cells may flow into fetal liver and colonize there through the interaction between Liv8/CD44 and HA.

In this study, we found that the expression of Liv8/CD44 decreased gradually during erythropoiesis (Fig. 3). Downregulation of CD44 was shown in human bone marrow cells during erythroid development and implicated in promotion of cell migration [20]. Therefore downregulation of Liv8/CD44 may contribute for de-adhesion and departure of hematopoietic cells from its niche in fetal liver.

CD44 was reported to be a signal transmitter into the cells, and a growth factor presentation molecule [21]. CD44 can be cleaved within the transmembrane domain leading to release of the CD44 cytoplasmic tail domain into the cytoplasm. The resulting CD44 cytoplasmic tail fragment translocate to the nucleus, where it can function as a transcriptional activator. It may be interesting Liv8/CD44 transmit signals to each other to control their proliferation and differentiation through down stream molecules or by itself. Moreover, CD44 was reported to act as a linker that connects membrane-type 1 matrix metalloproteinase (MT1-MMP), which degrades ECM barriers during cancer invasion, to the actin cytoskeleton and to play a role in directing MT1-MMP to the migration front. Therefore Liv8-antigen/CD44 may also contribute for ECM reconstruction that is needed to enter and create hematopoietic niche in fetal liver.

Recently, Kon et al. showed that CD44 is a specific marker of small hepatocytes, which are hepatic progenitor cells in adult liver, and its expression is upregulated at the time small hepatocytes start to proliferate both *in vitro* and *in vivo* [22]. Moreover preliminary data of the authors suggest that HA is important for the proliferation of small hepatocytes, but keeps them in their less differentiated state. Therefore Liv8/CD44 may play important role in the proliferation and/or differentiation of hepatic progenitor cells in both embryo and adult.

It was reported that stimulation by cytokines such as OSM, transforming growth factor β, Tumor necrosis factor α, IL-6 and IL-8 induce the expression of CD44 in various cells [23–25]. In our preliminary experiment, the expression of Liv8/CD44 did not differ significantly between WT and OSM receptor knockout fetal liver at E11.5. Therefore expression of Liv8-antigen/CD44 may not be induced by OSM, or another candidate factor(s) may function in combination with OSM and have a redundancy in the induction of Liv8-antigen/CD44. It is expected that further investigation of the molecular mechanisms underlying the induction of Liv8/CD44 in hepatoblasts.

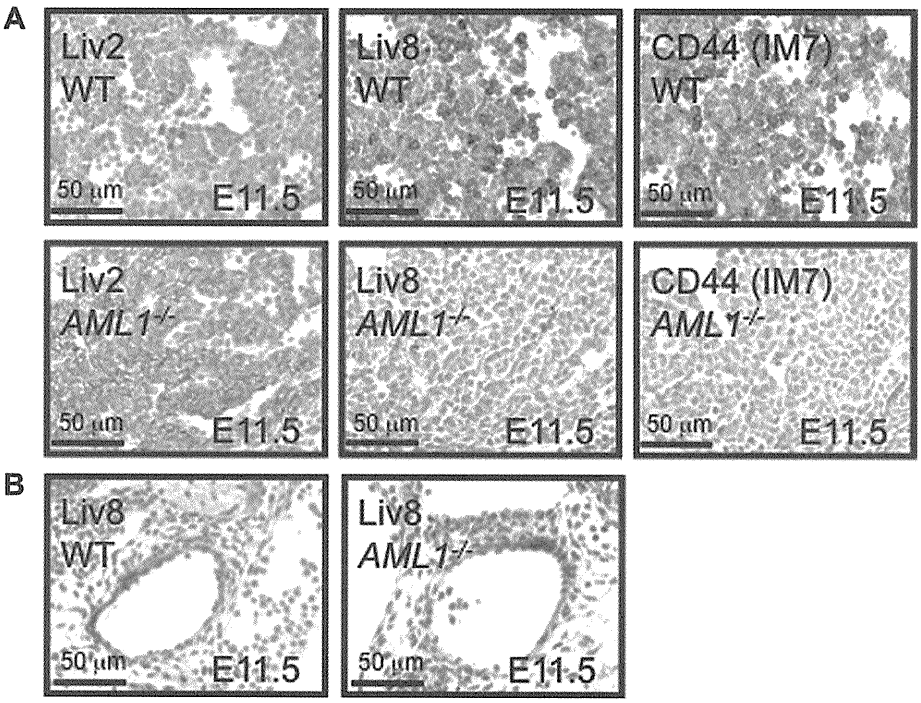

Fig. 4. Expression of Liv8/CD44 in WT and $AML^{-/-}$ fetal livers. (A,B) Transverse paraffin-sections of WT and $AML^{-/-}$ embryonic liver (A) and AGM region (B) at E11.5 were stained with anti-Liv2, anti-Liv8, and anti-CD44 (IM7) antibodies. Positive cells exhibit a brown precipitate. Nuclei were counterstained with hematoxylin (purple). Scale bars indicate 50 μm.

Acknowledgments

This work was supported in part by research grants (to H.N.) from the Ministry of Education, Culture, Sports, Science and Technology (MEXT) of Japan, and the Japan Society for the Promotion of Science (JSPS). We are grateful to Drs. Minoru Tanaka, Atsushi Miyajima, Yuki Nakayama, Takahiro Ito, and numerous members of the Nishina and Katada laboratories for critical reading and helpful discussions.

Appendix A. Supplementary data

Supplementary data associated with this article can be found, in the online version, at doi:10.1016/j.bbrc.2008.12.149.

References

[1] G. Keller, G. Lacaud, S. Robertson, Development of the hematopoietic system in the mouse, Exp. Hematol. 27 (1999) 777–787.
[2] M. Hata, M. Nanno, H. Doi, S. Satomi, T. Sakata, R. Suzuki, T. Itoh, Establishment of a hepatocytic epithelial cell line from the murine fetal liver capable of promoting hemopoietic cell proliferation, J. Cell. Physiol. 154 (1993) 381–392.
[3] M. Nanno, M. Hata, H. Doi, S. Satomi, H. Yagi, T. Sakata, R. Suzuki, T. Itoh, Stimulation of in vitro hematopoiesis by a murine fetal hepatocyte clone through cell–cell contact, J. Cell. Physiol. 160 (1994) 445–454.
[4] A. Kamiya, T. Kinoshita, Y. Ito, T. Matsui, Y. Morikawa, E. Senba, K. Nakashima, T. Taga, K. Yoshida, T. Kishimoto, A. Miyajima, Fetal liver development requires a paracrine action of oncostatin M through the gp130 signal transducer, EMBO J. 18 (1999) 2127–2136.
[5] T. Kinoshita, T. Sekiguchi, M.J. Xu, Y. Ito, A. Kamiya, K. Tsuji, T. Nakahata, A. Miyajima, Hepatic differentiation induced by oncostatin M attenuates fetal liver hematopoiesis, Proc. Natl. Acad. Sci. USA 96 (1999) 7265–7270.
[6] K.S. Zaret, Regulatory phases of early liver development: paradigms of organogenesis, Nat. Rev. Genet. 3 (2002) 499–512.
[7] A. Medvinsky, E. Dzierzak, Definitive hematopoiesis is autonomously initiated by the AGM region, Cell 86 (1996) 897–906.
[8] S. Hata, M. Namae, H. Nishina, Liver development and regeneration: from laboratory study to clinical therapy, Dev. Growth Differ. 49 (2007) 163–170.
[9] T. Watanabe, K. Nakagawa, S. Ohata, D. Kitagawa, G. Nishitai, J. Seo, S. Tanemura, N. Shimizu, H. Kishimoto, T. Wada, J. Aoki, H. Arai, T. Iwatsubo, M. Mochita, M. Satake, Y. Ito, T. Matsuyama, T.W. Mak, J.M. Penninger, H. Nishina, T. Katada, SEK1/MKK4-mediated SAPK/JNK signaling participates in embryonic hepatoblast proliferation via a pathway different from NF-kappa B-induced anti-apoptosis, Dev. Biol. 250 (2002) 332–347.
[10] T. Wada, N. Joza, H.M. Cheng, T. Sasaki, I. Kozieradzki, K. Bachmaier, T. Katada, M. Schreiber, E.F. Wagner, H. Nishina, J.M. Penninger, MKK7 couples stress signaling to G2/M cell cycle progression and cellular senescence, Nat. Cell Biol. 6 (2004) 215–226.
[11] I. Sakaida, S. Terai, N. Yamamoto, K. Aoyama, T. Ishikawa, H. Nishina, K. Okita, Transplantation of bone marrow cells reduces CCl4-induced liver fibrosis in mice, Hepatology 40 (2004) 1304–1311.
[12] N. Yamamoto, S. Terai, S. Ohata, T. Watanabe, K. Omori, K. Shinoda, K. Miyamoto, T. Katada, I. Sakaida, H. Nishina, K. Okita, A subpopulation of bone marrow cells depleted by a novel antibody, anti-Liv8, is useful for cell therapy to repair damaged liver, Biochem. Biophys. Res. Commun. 313 (2004) 1110–1118.
[13] H. Okada, T. Watanabe, M. Niki, H. Takano, N. Chiba, N. Yanai, K. Tani, H. Hibino, S. Asano, M.L. Mucenski, Y. Ito, T. Noda, M. Satake, AML1($^{-/-}$) embryos do not express certain hematopoiesis-related gene transcripts including those of the PU.1 gene, Oncogene 17 (1998) 2287–2293.
[14] T. Hara, Y. Nakano, M. Tanaka, K. Tamura, T. Sekiguchi, K. Minehata, N.G. Copeland, N.A. Jenkins, M. Okabe, H. Kogo, Y. Mukouyama, A. Miyajima, Identification of podocalyxin-like protein 1 as a novel cell surface marker for hemangioblasts in the murine aorta–gonad–mesonephros region, Immunity 11 (1999) 567–578.
[15] H. Kishimoto, K. Nakagawa, T. Watanabe, D. Kitagawa, H. Momose, J. Seo, G. Nishitai, N. Shimizu, S. Ohata, S. Tanemura, S. Asaka, T. Goto, H. Fukushi, H. Yoshida, A. Suzuki, T. Sasaki, T. Wada, J.M. Penninger, H. Nishina, T. Katada, Different properties of SEK1 and MKK7 in dual phosphorylation of stress-induced activated protein kinase SAPK/JNK in embryonic stem cells, J. Biol. Chem. 278 (2003) 16595–16601.
[16] A. Aruffo, I. Stamenkovic, M. Melnick, C.B. Underhill, B. Seed, CD44 is the principal cell surface receptor for hyaluronate, Cell 61 (1990) 1303–1313.
[17] J. Zhang, M. Socolovsky, A.W. Gross, H.F. Lodish, Role of Ras signaling in erythroid differentiation of mouse fetal liver cells: functional analysis by a flow cytometry-based novel culture system, Blood 102 (2003) 3938–3946.
[18] T. Okuda, J. van Deursen, S.W. Hiebert, G. Grosveld, J.R. Downing, AML1, the target of multiple chromosomal translocations in human leukemia, is essential for normal fetal liver hematopoiesis, Cell 84 (1996) 321–330.
[19] A. Avigdor, P. Goichberg, S. Shivtiel, A. Dar, A. Peled, S. Samira, O. Kollet, R. Hershkoviz, R. Alon, I. Hardan, H. Ben-Hur, D. Naor, A. Nagler, T. Lapidot, CD44 and hyaluronic acid cooperate with SDF-1 in the trafficking of human CD34+ stem/progenitor cells to bone marrow, Blood 103 (2004) 2981–2989.

[20] G.S. Kansas, M.J. Muirhead, M.O. Dailey, Expression of the CD11/CD18, leukocyte adhesion molecule 1, and CD44 adhesion molecules during normal myeloid and erythroid differentiation in humans, Blood 76 (1990) 2483–2492.
[21] H. Ponta, L. Sherman, P.A. Herrlich, CD44: from adhesion molecules to signalling regulators, Nat. Rev. Mol. Cell Biol. 4 (2003) 33–45.
[22] J. Kon, H. Ooe, H. Oshima, Y. Kikkawa, T. Mitaka, Expression of CD44 in rat hepatic progenitor cells, J. Hepatol. 45 (2006) 90–98.
[23] M. Barshishat, A. Ariel, L. Cahalon, Y. Chowers, O. Lider, B. Schwartz, TNFalpha and IL-8 regulate the expression and function of CD44 variant proteins in human colon carcinoma cells, Clin. Exp. Metastasis 19 (2002) 327–337.
[24] J. Cichy, E. Pure, Oncostatin M and transforming growth factor-beta 1 induce post-translational modification and hyaluronan binding to CD44 in lung-derived epithelial tumor cells, J. Biol. Chem. 275 (2000) 18061–18069.
[25] T. Vincent, N. Mechti, IL-6 regulates CD44 cell surface expression on human myeloma cells, Leukemia 18 (2004) 967–975.

Hepatology Research 2009; 39: 633–644 doi: 10.1111/j.1872-034X.2009.00522.x

Review Article

Liver development: lessons from knockout mice and mutant fish

Takashi Nakamura and Hiroshi Nishina

Department of Developmental and Regenerative Biology, Medical Research Institute, Tokyo Medical and Dental University, Yushima, Bunkyo-ku, Tokyo, Japan

The liver is an organ with vital functions, including the processing and storage of nutrients, maintenance of serum composition, detoxification and bile production. Over the last 10 years, there have been major advances in our understanding of the molecular and cellular mechanisms underlying liver development. These advances have been achieved through the use of knockout mice as well as through forward-genetics studies employing mutant fish. The examination of many such murine and piscine mutants with defects in liver formation and/or function have pinpointed numerous factors crucial for hepatic cell differentiation and growth. In addition, these studies have permitted the identification of several important liver-specific markers that allow the contributions of variouscell types to hepatogenesis to be monitored. This review summarizes our current state of knowledge of the shared molecular mechanisms that underlie liver development in species as diverse as fish and mice. A better molecular understanding of liver formation may provide new insights into both normal liver biology and liver disease.

Key words: antibody, knockout mice, liver development, medaka, zebrafish

INTRODUCTION

THE LIVER PLAYS a central role in metabolic homeostasis because this organ is responsible for the metabolism, synthesis, storage and redistribution of nutrients such as carbohydrates, fats and vitamins. The liver is also the main detoxifying organ of the body, removing waste and xenobiotics through metabolic conversion and biliary excretion. Most of these functions are carried out by hepatocytes and bile duct cells. The common progenitor of these cell types, the hepatoblast, arises during early embryogenesis at a specific location in the embryonic endoderm. Hepatoblasts go on to either self-renew or proliferate and differentiate into hepatocytes and bile duct cells under the influence of a wide spectrum of genes.[1–3] Owing to the essential nature of liver functions, mutation of many of these genes results in embryonic lethality, which makes it difficult to use genetic screening to isolate developmental mutants with liver defects. Instead, reverse-genetics studies using mice and forward-genetics approaches using small aquarium fish such as zebrafish and medaka have been successfully employed to reveal much information about regulatory genes that are crucial for liver development (Table 1). Another barrier to analyzing mechanisms of liver development has been a dearth of liver-specific markers. However, in recent years, several molecules that are expressed specifically in fetal liver cells have been identified. In this review, we discuss several important molecular aspects of liver development as revealed by the use of these markers and mutants.

Correspondence: Professor Hiroshi Nishina, Department of Developmental and Regenerative Biology, Medical Research Institute, Tokyo Medical and Dental University, 1-5-45 Yushima, Bunkyo-ku, Tokyo 113-8510, Japan. Email: nishina.dbio@mri.tmd.ac.jp
Received 20 January 2009; revision 11 February 2009; accepted 18 February 2009.

STAGES OF LIVER DEVELOPMENT

EMBRYONIC LIVER DEVELOPMENT occurs in multiple stages that are governed by hormonal factors as well as by intercellular and matrix–cellular interactions. In mice, liver ontogeny initiates around embryonic day 9 (E9), when epithelial cells of the foregut endoderm interact with the cardiogenic mesoderm and commit to becoming the liver primordium[4] (Fig. 1). The liver primordium proliferates and invades the mesenchyme of the septum transversum to give rise to the hepatic codes

Table 1 Genes and mutations affecting liver formation and function

Mouse		
Genes	Description	Knockout mouse liver phenotype
Bmp4	TGF-β family	Delayed growth of the hepatic bud, defect in hepatoblast proliferation
Hhex	Transcriptional repressor	Defect in hepatoblast differentiation, lack of Hnf4α Hnf6 expression
RelA	NF-κB subunit	Massive liver degeneration and apoptosis
Ikkβ	NF-κB signaling molecule	Massive liver degeneration and apoptosis
NEMO	NF-κB signaling molecule	Massive liver degeneration and apoptosis
Tbk1	NF-κB signaling molecule	Massive liver degeneration and apoptosis
Pik3r1	PI3-kinase subunits	Hepatocyte necrosis
Mkk4	MAPKK	Impaired hepatoblast proliferation
Mkk7	MAPKK	Impaired hepatoblast proliferation
c-jun	AP-1 transcription factor	Defect in liver development
Tbx3	T-box transcription factor	Impaired hepatoblast proliferation
Hlx	Homeobox transcription factor	Impaired hepatic development
Xbp1	X-box transcription factor	Hypoplastic fetal liver
C/EBPα	Transcription factor	Failure of normal liver development
K-ras	GTPase	Defect in the fetal liver microenvironment
Hnf6	Transcription factor	Absence of hepatic artery branches
Zebrafish		
Mutation	Description	Liver phenotype
prometheus (Wnt2bb)	Wnt2bb	Defects in liver specification
Medaka		
Genes		Liver phenotype
hirame	Not identified	Defect in hypoblast convergence
fukuwarai	Not identified	Absence of the hepatic bud
sakura	Not identified	Absence of the hepatic bud
mochizuki	Not identified	Lack of foxA3 expression
akatsuki	Not identified	Lack of foxA3 expression
akebono	Not identified	Lack of foxA3 expression
kakurenbo	Not identified	Small and mislocated liver
hiohgi	Not identified	Small liver
kamifusen	Not identified	Malformed liver
origami	Not identified	Malformed liver
kendama	Not identified	Inverted positions of liver and gall bladder
dendendaiko	Not identified	Inverted positions of liver and gall bladder
hanetsuki	Not identified	Inverted positions of liver and gall bladder
akane	Not identified	Deep red bile
suou	Not identified	Light red bile
ominaeshi	Not identified	Colorless bile
ukon	Not identified	Failure to metabolize PED6 (phospholipase A2 substrate)
aonibi	Not identified	Failure to metabolize PED6 (phospholipase A2 substrate)
uguisucha	Not identified	Failure to metabolize PED6 (phospholipase A2 substrate)

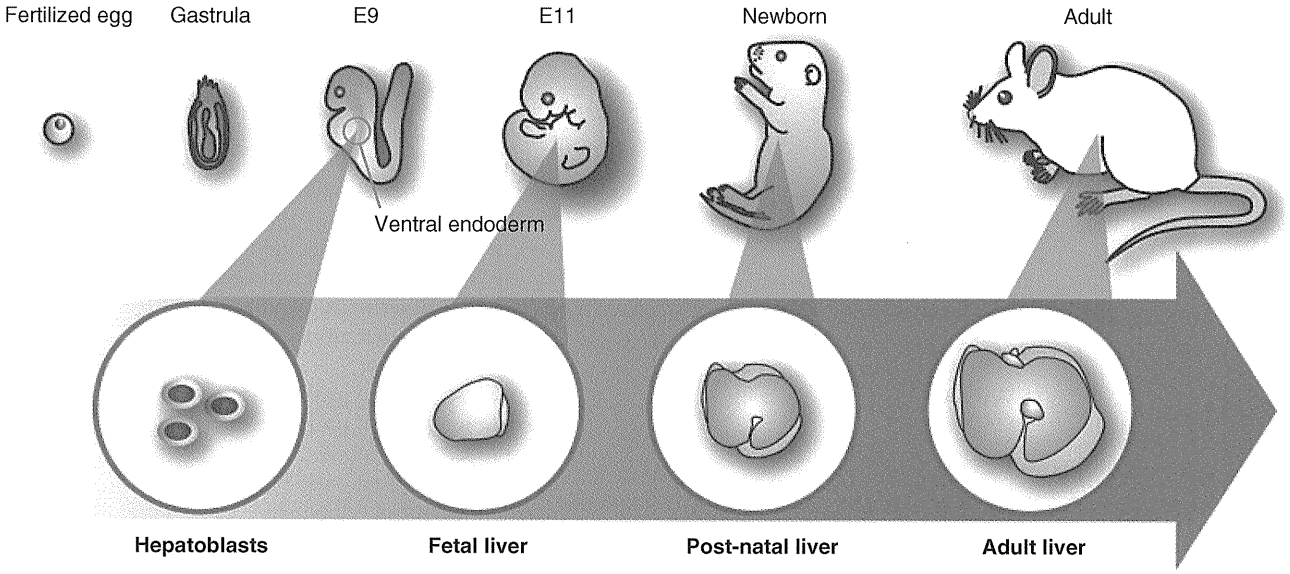

Figure 1 Overview of the stages of murine liver development. The fertilized egg develops into embryo through gastrulation and organogenesis begins. By embryonic day 9 (E9), the ventral endoderm generates hepatoblasts. By E11, the fetal liver forms and becomes the major site of hematopoiesis. After birth, the post-natal liver functions mainly in metabolism, a capacity maintained in the adult.

and hepatic bud at E9.5. At E10.5–12.5, the fetal liver takes over hematopoiesis from the yolk sac and aorta–gonad–mesonephros (AGM) region. This switch in hematopoietic organ represents a critical checkpoint in murine embryogenesis. The next major stage of liver development occurs around E14.5 when bipotential hepatoblasts present in the hepatic bud differentiate into hepatocytes and bile duct cells.[5,6] These cells continue to proliferate and eventually cooperate to form the post-natal liver. The liver's main function then switches from hematopoiesis to metabolism, a function that also dominates in the adult liver.

KNOCKOUT MOUSE MODELS OF LIVER DEVELOPMENT

A VARIETY OF knockout mouse models have been used to elucidate different aspects of liver development, including: (i) the development of hepatoblasts from multipotential endodermal stem cells; (ii) the survival and proliferation of hepatoblasts; and (iii) the differentiation of bile duct cells and hepatocytes from hepatoblasts (Fig. 2). Fibroblast growth factors (FGF) and bone morphogenic proteins (BMP) are essential for hepatic bud formation and for the development of hepatoblasts from endodermal stem cells. For example, mice deficient for BMP-4 exhibit delayed growth of the hepatic bud.[7] Homeobox genes are also critical, as the endoderm-specific homeobox gene, *Hhex*, has been found to be essential for proper hepatoblast differentiation. *Hhex* is expressed in the endoderm before liver induction and is necessary for the expression of other genes involved in liver development.[8–10] In *Hhex* knockout mice, expression of the *Hnf4α* and *Hnf6* genes, which are required for the differentiation of bile duct cells and hepatocytes from hepatoblasts, is lost.[11]

Tumor necrosis factor-α (TNF-α) is an inflammatory cytokine that elicits a wide range of biological responses, including tumor necrosis, inflammation, cellular differentiation, proliferation and apoptosis (Fig. 3). In the fetal liver, TNF-α engagement of TNF receptor 1 (TNFR1) activates three separate signaling pathways: (i) activation of a cell death signal; (ii) activation of NF-κB signaling that opposes the cell death signal and guarantees cell survival; and (iii) activation of stress-activated protein kinase (SAPK)/c-Jun N-terminal kinase (JNK) signaling that induces cell proliferation. Knockout mice lacking genes involved in NF-κB signaling are embryonic lethal and exhibit massive liver degeneration and apoptosis during midgestation at E12.5–16. Examples include mice deficient for the RelA subunit of transcription factor nuclear factor-κB (NF-κB) (die at E15–16),[12] IKKβ (die at E12.5–14),[13–15] NEMO (die at E12.5–13.0),[16] or TANK-

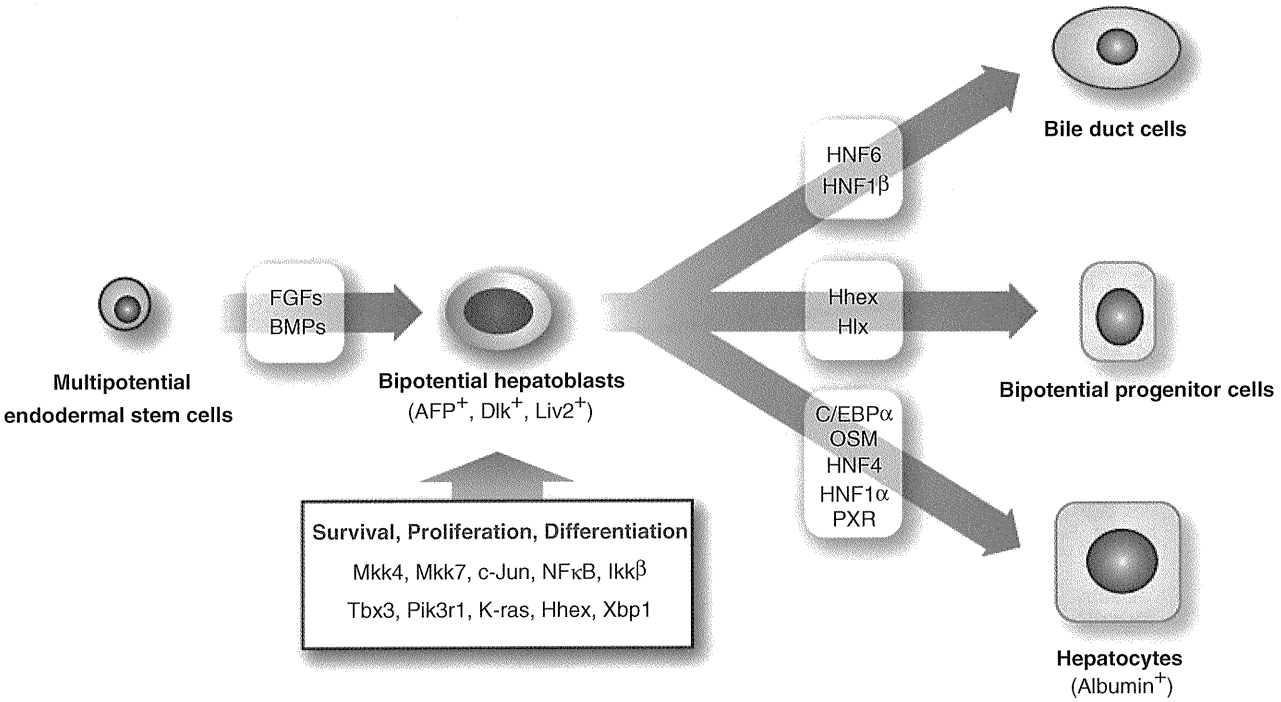

Figure 2 Factors influencing the development, survival, proliferation and differentiation of murine hepatic cells. Under the influence of fibroblast growth factors (FGF) and bone morphogenic proteins (BMP), multipotential endodermal stem cells generate bipotential hepatoblasts. Under the influence of the indicated genes, the hepatoblasts either self-renew or differentiate into bile duct cells and hepatocytes. Many of the indicated factors are discussed in the text. See Table 1 for information on other markers. AFP, α-fetoprotein.

binding kinase (TBK1; die at E12.5–14.5).[17] Importantly, the embryonic lethality and liver cell death observed in RelA-, IKKβ- or TBK1-deficient embryos can be rescued by the simultaneous inactivation of TNFR1. These results suggest that developing liver cells are routinely exposed to TNF-α produced by hematopoietic cells, and that the death signaling mediated by TNF-α must be countered by NF-κB signaling to ensure continued liver development. Another gene required for hepatocyte survival is *Pik3r1*, which encodes regulatory subunits of phosphoinositide-3-kinase (PI3K). Knockout mice lacking Pik3r1 expression show massive hepatocyte death and perinatal lethality.[18]

c-Jun N-terminal kinase is primarily activated in response to a variety of cellular stresses, including metabolic poisons, DNA damage, changes in osmolarity, heat shock, and the presence of the inflammatory cytokines interleukin (IL)-1 and TNF-α. Activated JNK phosphorylates c-Jun and thereby promotes the formation of the c-Jun/Fos heterodimer that constitutes the AP-1 transcriptional complex, which is a key regulator of gene expression. JNK is also directly activated by MKK4 (also called SEK1) and MKK7, which are activated in response to the binding of hepatocyte growth factor (HGF) to its receptor c-Met. We and several other groups have used gene-targeting to disrupt the *Mkk4* gene in mice and have found that MKK4-deficient embryos display severe anemia and die at E10.5–12.5.[19–23] Although vasculogenesis and hematopoiesis from yolk sac precursors are normal in MKK4-deficient embryos, liver formation is severely impaired. Hepatocyte numbers are greatly reduced in MKK4-deficient embryos due to massive hepatoblast apoptosis at E12.5. Embryos with a disrupted *c-jun* gene also display defective liver organization and die at E11.5–15.5.[24,25] MKK7-deficient mice show impaired liver formation at E11.5–12.5 as well as reduced c-Jun phosphorylation and decreased expression of the G2/M cell-cycle kinase Cdc2.[26] This latter result indicates that JNK signaling leading to c-Jun phosphorylation and thus Cdc2 regulation is vital for hepatoblast proliferation in the developing liver.

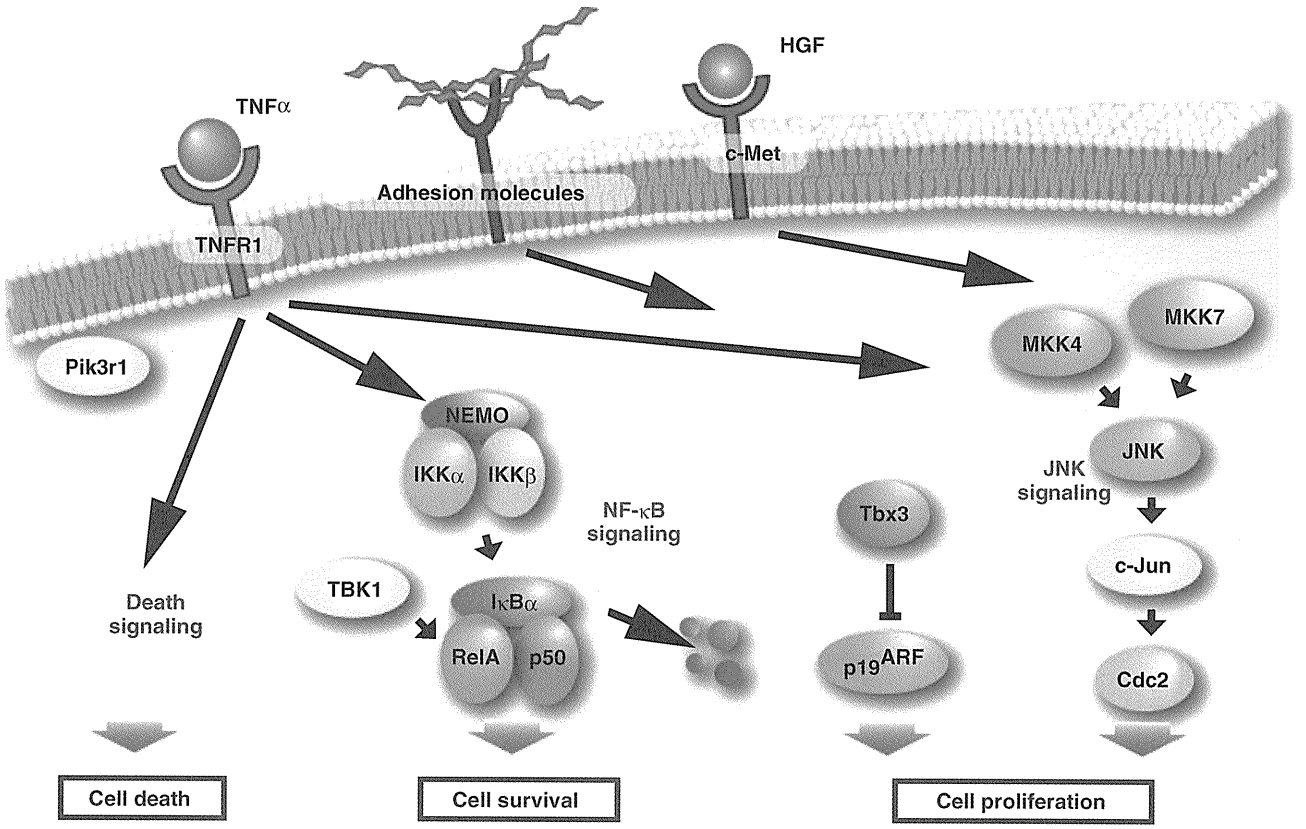

Figure 3 A proposed model for signaling pathways in murine hepatoblasts. Engagement of tumor necrosis factor-α engagement of TNF receptor 1 (TNFR1) by tumor necrosis factor-α elicits a wide range of biological responses, including cell death, survival and proliferation. In hepatoblasts, the induction of cell-death signaling, nuclear factor-κB (NF-κB) activation and c-Jun N-terminal kinase (JNK) activation are simultaneously mediated through TNFR1. JNK is also activated by the binding of hepatocyte growth factor (HGF) to its receptor c-Met. NF-κB activation requiring all the signaling elements shown here protects hepatoblasts against cell death, whereas JNK activation leading to c-Jun phosphorylation and *cdc2* gene expression drives cell proliferation. The Tbx3 transcription factor suppresses $p19^{ARF}$ expression, allowing hepatoblast proliferation and, subsequently, differentiation.

Another transcription factor important for liver development is the T-box gene, *Tbx3*. *Tbx3* is the first T-box gene implicated in yolk sac development, and mutations in this gene cause Ulnar-Mammary syndrome. Knockout mice lacking *Tbx3* exhibit embryonic lethality at E12.5 due to impaired yolk sac formation.[27] *Tbx3* also controls the fate of hepatoblasts during liver development, because Tbx3-deficient hepatoblasts show severe defects in proliferation and are abnormally biased towards bile duct cell differentiation.[28] At the molecular level, deletion of *Tbx3* results in increased expression of the tumor suppressor $p19^{ARF}$, which in turn induces growth arrest in hepatoblasts and activates the bile duct cell differentiation program. Thus, *Tbx3* plays an important role in controlling the proliferation and cell-fate determination of hepatoblasts by suppressing $p19^{ARF}$ expression.

MUTANT FISH MODELS OF LIVER DEVELOPMENT

OVER THE LAST decade, studies in rats and mice have greatly expanded the list of molecules known to contribute to liver development. However, identification of novel factors using mammalian model organisms is inefficient and expensive compared with studies of other vertebrate model organisms such as zebrafish (*Danio rerio*) and medaka (*Oryzia latipes*). These small

fish can be bred in large numbers and require little cost and effort to maintain. High-throughput screens based on these models are already yielding a wealth of new information on liver gene functions.[29] In zebrafish, random chemical mutagenesis mediated by *N*-acethyl *N*-nitrosourea (ENU) treatment is widely used in forward-genetics screening (Fig. 4). Another approach is to carry out ENU-mediated mutagenesis of a transgenic

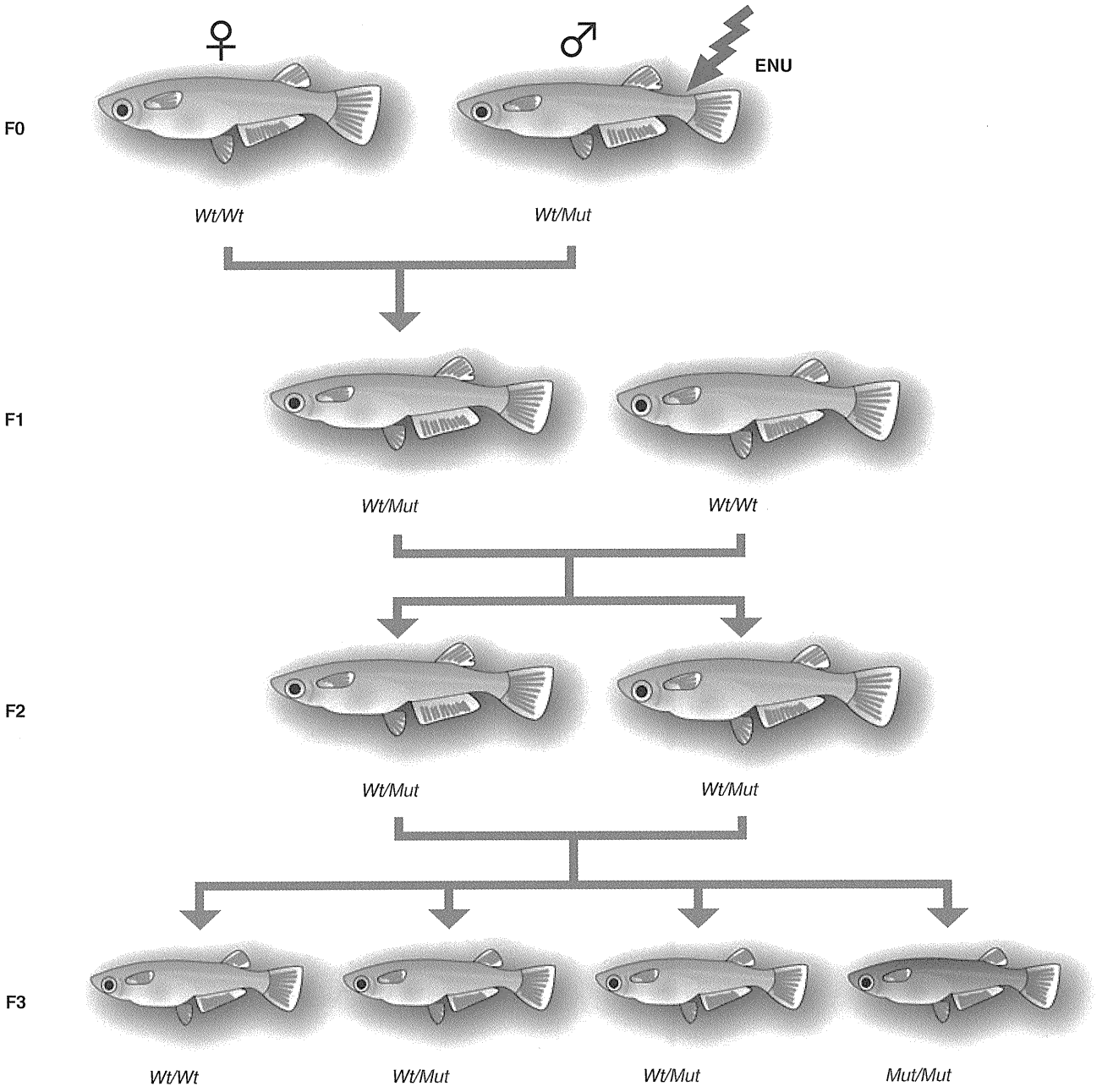

Figure 4 Scheme illustrating the mutagenesis and breeding of small fish to identify recessive mutations. Male fish are treated with *N*-acethyl *N*-nitrosourea (ENU) to induce point mutations (*Mut*) in the germline. The treated males are bred to untreated, wild-type females (*Wt*) to fix the mutations in the resulting progeny. The F_1 progeny are bred with Wt fish and the resulting F_2 progeny are intercrossed. The F_3 clutches contain 25% phenotypically abnormal offspring.